Chimica et Natura Acta
p-ISSN: 2355-0864 e-ISSN: 2541-2574
Homepage: http://jurnal.unpad.ac.id/jcena

Plasmonic Sensor Nata de Coco Film Inserted with Copper Nanoparticles for Detection of Mercury by UV-Vis Spectrophotometry

Abdul Haris Watoni*, Rijal Rijal, La Ode Ahmad Nur Ramadhan, La Ode Abdul Kadir

Department of Chemistry, Mathematics and Natural Sciences, Halu Oleo University, Indonesia
*Corresponding author: ahwatoni@gmail.com

DOI: https://doi.org/10.24198/cna.v13.n1.54839

Abstract: The rapid development of the mining industry has resulted in an increasing amount of toxic waste materials in the environment, including mercury (Hg). A reliable chemical sensor is needed to detect the presence of mercury. One of the chemical sensors that is starting to be widely developed is plasmonic film. This research aims to determine the characteristics and validity of plasmonic *nata de coco*-copper nanoparticle (CuNPs) films for cuvette type sensor chips in the rapid detection of Hg metal using UV-Vis spectrophotometry. This research began with the preparation of a bioreductor from red dragon fruit peel extract, green synthesis of CuNPs, synthesis of *nata de coco*, and synthesis of *nata de coco*-cellulose plasmonic film inserted with CuNPs-red dragon fruit peel extract. The next stage is the validation and application of plasmonic films for Hg metal detection using UV-Vis spectrophotometry. The success of this research was proven through characterization using an Ultra Violet-Visible (UV-Vis) spectrophotometer, a Fourier Transform Infra Red (FTIR) spectrophotometer, and a digital optical microscope. UV-Vis spectrophotometric analysis showed the formation of stable CuNPs with a diameter of 46 nm – 92 nm. FTIR analysis shows changes in functional groups in the red dragon fruit peel extract compound, *nata de coco* cellulose, and the formation of Cu-O bonds as an indication that the process of reducing Cu^{2+} ions to Cu^{0} has occurred and the insertion of CuNPs-red dragon fruit peel extract in the *nata de coco* cellulose film matrix. Analysis using an optical microscope shows the morphology of CuNPs with a uniform round shape. Measurement of the Hg standard solution using UV-Vis spectrophotometry in a cuvette inserted with a plasmonic film has good accuracy and precision with %*R* = 103.9% and %*RSD* = 0.9%, with LOD and LOQ values of 0.193 ppm and 0.245 ppm, respectively. The use of plasmonic film in determining Hg using UV-Vis spectrophotometry was proven more sensitive than without plasmonic film with a sensitivity value of 1.50. These results indicate that the pasmonic film from *nata de coco*-CuNPs has the potential to be applied as a cuvette type sensor chip for Hg metal detection.

Keywords: plasmonic film, *nata de coco*, CuNPs, mercury (Hg), cuvette type sensor

***Abstrak*:** Perkembangan industri pertambangan yang pesat menyebabkan semakin banyaknya bahan buangan beracun di lingkungan, termasuk logam merkuri (Hg). Untuk mendeteksi keberadaan merkuri diperlukan sensor kimia yang handal. Salah satu sensor kimia yang mulai banyak dikembangkan adalah film plasmonik. Tujuan penelitian ini adalah untuk mengetahui karakteristik dan menentukan validitas film plasmonik *nata de coco*-nanopartikel tembaga (CuNPs) untuk chip sensor tipe *cuvette* pada deteksi cepat logam Hg secara spektrofotometri UV-Vis. Penelitian ini diawali dengan penyiapan bioreduktor ekstrak kulit buah naga merah, green sintesis CuNPs, sintesis *nata de coco*, dan sintesis film plasmonik selulosa *nata de coco* terinsersi CuNPs-ekstrak kulit buah naga merah. Tahap berikutnya adalah validasi dan penerapan film plasmonik untuk deteksi logam Hg secara spektrofotometri UV-Vis. Keberhasilan penelitian ini dibuktikan melalui karakterisasi menggunakan spektrofotometer *Ultra Violet-Visible* (UV-Vis), spektrofotometer *Fourier Transform Infra Red* (FTIR), dan mikroskop optik digital. Analisis secara spektrofotometri UV-Vis menunjukkan terbentuknya CuNPs yang stabil dengan diameter 46 nm – 92 nm. Analisis FTIR menunjukkan perubahan gugus fungsi dalam senyawa ekstrak kulit buah naga merah, selulosa *nata de coco*, dan terbentuknya ikatan Cu-O sebagai indikasi telah terjadinya proses reduksi ion Cu^{2+} menjadi Cu^{0} dan terinsersinya CuNPs-ekstrak kulit buah naga merah dalam matriks film selulosa *nata de coco*. Adapun analisis menggunakan mikroskop optik memperlihatkan morfologi CuNPs dengan bentuk bulat seragam. Pengukuran larutan standar Hg secara spektrofotoketri UV-Vis dalam kuvet terinsersi film plasmonik memiliki akurasi dan presisi yang baik dengan %*R* = 103.9% dan % *RSD* = 0.9%, dengan nilai LOD serta LOQ berturut-turut 0,193 ppm dan 0.245 ppm. Penggunaan film plasmonik dalam penentuan Hg secara spektrofotometri UV-Vis terbukti lebih sensitif dibandingkan tanpa film plasmonik dengan nilai sensitivitas 1.50. Hasil tersebut menunjukkan bahwa film pasmonik dari *nata de coco*-CuNPs berpotensi untuk diaplikasikan sebagai chip sensor tipe *cuvette* pada deteksi logam Hg.

Kata kunci: *film plasmonik, nata de coco, CuNPS, merkuri (hg), sensor tipe cuvette.*

INTRODUCTION

The increasingly rapid development of the mining industry has resulted in more toxic waste materials being dumped into the environment. Mining activities produce waste which is dangerous for the continuity of an ecosystem, because it contains heavy metals such as Cu, Zn, Pb and Hg (Miftahurrahmah *et al*. 2017). The presence of mercury (Hg) in the environment generally due to waste of the gold mining and oil drilling industries, which pollute the environment. Mercury metal compounds are often found in leachate at landfills, scrubber water from incinerators, metal plating wastewater, electronic component washing industries, laboratory wastewater, and others. These heavy metals accumulate in the environment, especially settling at the bottom of waters and forming complex compounds with organic and inorganic materials (Setiyono & Annisa 2012). In addition, Hg can enter the human body through the skin, breathing and digestion (Al-Ayubi *et al*. 2010). Hg can also accumulate in water microorganisms through metabolic processes. Materials containing Hg thrown into rivers or the sea will be consumed by microorganisms and chemically transformed into methylmercury compounds, which accumulate in the human body through the food chain (Silalahi *et al*. 2012). To monitor the presence of Hg, a reliable detection tool is needed. A chemical sensor is one technology that enables the detection of mercury.

A chemical sensor is an analytical device that contains chemical reagents that can react with specific analytes in solution or gas to produce physical and chemical changes that can be modified (physicochemical transducer) into proportional electrical signals. Many chemical sensors are costly and are limited to responding to color changes only. One of the many chemical sensors developed uses a fluorescent signal on a sol-gel membrane, but this method requires complicated membrane preparation. Therefore, it is necessary to explore more practical methods like plasmonic sensors, which are able to determine the concentration of analytes in samples, provide a fast response, and efficient (Amaliyah *et al*. 2021).

Plasmonic film sensor that can be applied to cuvette cells which allows UV-Vis spectrophotometric detection. Research related to plasmonic sensors in cuvette cells was previously studied by Oh *et al*. (2019) using test samples of baby milk containing melamine, but this research used glass film as a substrate. Glass substrates have the potential to become new waste in the environment. Therefore, it is necessary to update by applying the natural polymer of bacterial cellulose as an environmentally friendly porous substrate in making cuvette-type sensor chips. One material that meets these criteria is *nata de coco* inserted with green copper nanoparticles (CuNPs).

A stabilizer or capping agent is generally required for nanoparticle synthesis. The stabilizer materials that are widely used are synthetic polymers, however, these polymers can cause environmental problems, so it is necessary to find a solution to use environmentally friendly capping agents (Salasa *et al*. 2016). Plant extracts can be used as bioreductors to replace chemical reducing agents, as well as capping agents because plant extracts contain secondary metabolite compounds which can stabilize free radicals by preventing chain reactions (Wisnuwardhani *et al*. 2019). Red dragon fruit peel extract is one of the plants that can be used as a bioreductor, because red dragon fruit peel contains antioxidants such as vitamin C, flavonoid compounds, and polyphenols that have the potential to act as bioreductors (Yanti & Siska 2017). Therefore, green CuNPs can be synthesized using red dragon fruit peel extract. The synthetic product is called CuNPs-red dragon fruit peel extract. CuNPs-red dragon fruit peel extract can be inserted into *nata de coco* to form a plasmonic film for heavy metal detection. The use of *nata de coco* is considered effective because it has many advantages, including being reversible, drying quickly, easy to apply, and safe to use for detecting heavy metal content in the environment (Boby *et al*. 2021).

Nata de coco can be produce by enzymatic method using *Acetobacter xylinum* bacteria. The presence of a starter plays an important role in increasing the number of *Acetobacter xylinum* colonies that produce nata-forming enzymes. Referring to the research of Dirpan *et al*. (2019), the addition of vinegar aims to regulate the acidity or pH level to suit the characteristic conditions for optimum growth of *Acetobacter xylinum* bacteria, namely pH 4 and 5 at a temperature of 28℃ – 30℃. The formation of cellulose in the fermentation process begins with the appearance of thread-like fibers which then change shape into cellulose ropes like woven cellulose known as nata (Putri *et al*. 2021). The *nata de coco* formed is composed of a network of microfibrils. The membrane is formed as a result of a series of activities of the *Acetobacter xylinum* bacteria with the nutrients in the liquid media. Glucose nutrition is found in coconut water and granulated sugar. Glucose is formed by the hydrolysis reaction of sucrose with water in granulated sugar. The glucose involved in the formation of cellulose is β-glucose. α-Glucose is converted into β form by the isomerase enzyme in the *Acetobacter xylinum* bacteria. The change in β form occurs in the –OH group on the C-1 atom (Figure 1 (a). Next, glucose will bond with other glucose via a 1,4-β-glycoside bond. This bond occurs between the –OH group on the C-1 atom from one β-glucose with

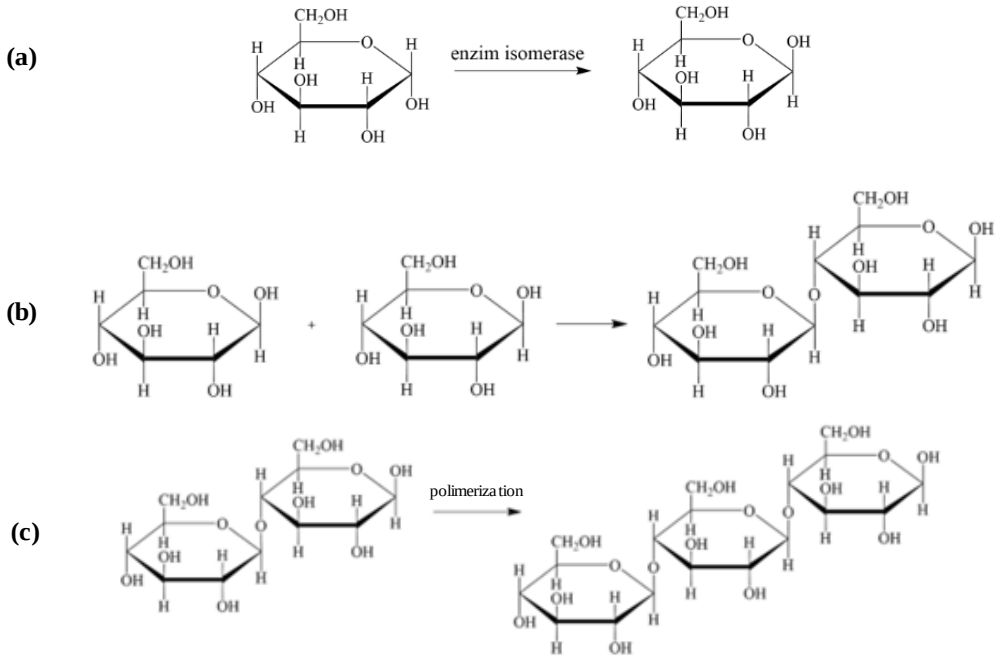

Figure 1 Polymerization reaction in the formation of *nata de coco* cellulose. (a) The reaction of changing α-glucose to β-glucose by the isomerase enzyme, (b) the reaction of forming disaccharides with glycosidic bonds, and (c) the polymerization reaction of disaccharides into the cellulose part of *nata de coco*.

the –OH group on the C-4 atom of the other β-glucose (Figure 1 (b)). Different thicknesses at varying incubation times are related to the polymerization process. CuNPs-inserted *nata de coco* film can be applied as a plasmonic film to detect the presence of heavy metal in samples by UV-Vis spectrophotometry. However, there has been no information regarding the optimum thickness of the film to detect heavy metals using this method.

In UV-Vis spectroscopic heavy metal detection, a cuvette-type plasmonic film can be applied directly to the cuvette as a substitute for the measured aqueous sample. Metal nanoparticles are added to the film to help speed up the detection of heavy metals such as mercury. The application of metal nanoparticles in chemical sensors refers to the surface plasmon resonance (SPR) properties of the nanoparticles, namely the resonant interaction of electron bands on the surface of the nanoparticle when exposed to light. According to Rahmawati *et al*. (2020), this absorption occurs in Au, Ag, and Cu nanoparticles. The use of nanoparticles aims to increase the coloring and detection sensitivity of cuvette-type plasmonic sensors, so this nanomaterial is expected to be a new alternative to replace colorimetric reagents which are quite expensive.

Based on the study above, in this study has been carried out on the synthesis and characterization of *nata de coco* plasmonic films inserted with CuNPs-red dragon fruit peel extract for cuvette-type sensor chips as a detector for the heavy metal Hg content. In this article, we reported the results of the synthesis and characterization of CuNPs-red dragon fruit extract, synthesis of *nata de coco* film, and validation of the *nata de coco*-CuNPs-red dragon fruit extract composite film for cuvette type sensor chips for rapid detection of the heavy metal mercury.

MATERIALS AND METHODS

Materials

The materials used in this research were distilled water (H_2O), copper sulfate ($CuSO_4$), 96% ethanol (C_2H_5OH), glacial acetic acid (CH_3COOH), sodium hydroxide (NaOH), glucose ($C_6H_{12}O_6$), Zwavelzure ammonium (ZA), *Acetobacter xylinum* seed starter, coconut water (Cocos nucifera), red dragon fruit peel (Hylocereus polyrhizus), newsprint, rubber bands, Whatmann no. 42 filter paper, label paper, tissue, plastic wrap and aluminum foil. The equipments used were beakers-250, 500, and 1000 mL (Iwaki Pyrex), measuring cylinders-10, 50 and 100 mL (Iwaky Pyrex), measuring flasks-100 and 250 mL (Iwaki Pyrex), oven (Gallenkamp England), pipettes drops, hot plate, vial, dark bottle, stir bar, spray bottle, analytical balance, spatula, funnel, petri dish (Iwaki Pyrex), knife, blender, filter, jar, cuvette, Hidroulic Power Press, desiccator, centrifuge, stirrer magnetic, rotary evaporator, Bunsen burner, micropipette, Laminar Air Flow, Fourier Transform Infrared (FTIR) (Shimadzu), UV-Vis Spectrophotometer (Spectroquant Pharo 300 M), and digital optical microscope.

Synthesis of Nata de Coco

Put 1 liter of clean coconut water into a sterile container, then add 100 g of granulated sugar and 15

g of ZA. The mixture is then heated until it boils to kill the microorganisms in the coconut water. The boiled coconut water is then cooled and 10 mL of glacial acetic acid is added to 250 mL of *Acetobacter xylinum* inoculum solution. The fermentation medium is then poured into a sterile container for two hours until the temperature reaches room temperature. The media placed in a container is then covered with newspaper and fermented for ten days (Hasriana 2021). *Nata de coco* was further characterized before being used as a film matrix.

Extraction of Red Dragon Fruit Skin (*Hylocereus polyrhizus*)

The extraction of red dragon fruit skin was adapted from research by Widianingsih (2016) through a maceration process using 96% ethanol solvent. A total of 500 g of red dragon fruit peel was macerated using 1 L of 96% ethanol, left for 3×24 hours while stirring twice a day, then filtered to separate the filtrate and residue. The extract liquid is then concentrated using a rotary evaporator at 50℃ for 3 hours and then heated in an oven at 50℃ for 30 minutes to remove the water. The extraction process is stopped when equilibrium has been reached between the compounds in the solvent and the compounds in the plant cells.

Synthesis of Copper Nanoparticles (CuNPs)-Red Dragon Fruit Peel Extract

The synthesis of copper nanoparticles was adapted from research by Laila *et al*. (2021) using the green synthesis method. A solution of 0.1 M $CuSO_4$ precursor and red dragon fruit peel extract was put into a beaker with a ratio of 1:1, 1:2, 1:3, 1:4, 1:5, and 1:6 (v/v). In each composition, the volume of precursor solution used is 5 mL. The mixture was then stirred using a magnetic stirrer for 2 hours and centrifuged at 3,000 rpm for 30 minutes. The filtrate resulting from centrifugation is put into a vial that has been labeled with the mixture composition. The precipitate was then dried in an oven at 50℃ for 1 hour until a shiny black powder was obtained which was ready to be characterized.

Synthesis of Plasmonic Film Nata de coco-CuNPs-Red Dragon Fruit Peel Extract

Clean *nata de coco* is soaked in 2% (w/v) sodium hydroxide solution so that multiplying the *Acetobacter xylinum* bacteria and the formation of nata can stop. Next, rinse the *nata de coco* using distilled water until the pH is neutral. The *nata de coco* is then pressed using a Hidroulic Power Press into a thin film sheet with a thickness of 0.05 cm. This film is then cut to a size of 5 cm × 1 cm and soaked in epoxy resin to form a transparent thin film, then dried. The dried film was then soaked in a suspension of CuNPs-red dragon fruit peel extract for 5 minutes. Finally, the film that had been inserted with CuNPs-red dragon fruit peel extract was dried to obtain a plasmonic film that was ready to be characterized and used for measuring mercury in aqueous samples. Based on the composition of the precursor: bioreductor used for the synthesis of CuNPs-dragon fruit peel extract, the *nata de coco* film inserted with CuNPs-dragon fruit peel extract obtained is referred as plasmonic film-1:1, 1:2, 1:3, 1:4, 1:5, and 1:6.

Characterization

The success of the synthesis of *nata de coco*, CuNPs-red dragon fruit peel extract, and plasmonic films of *nata de coco*-CuNPs-red dragon fruit peel extract were characterized using FTIR, UV-Vis spectrophotometer, and digital optical microscopy. Characterization using FTIR aims to determine the presence of functional groups and indications of their changes. Analysis using FTIR was carried out on each deposit of CuNPs-red dragon fruit peel extract obtained. A sample of CuNPs powder-red dragon fruit peel extract was mixed with a KBr plate and made into pellets. Spectrum recording was carried out at room temperature with a resolution of 8.0 cm^{-1} in the wave number range of 4000 – 450 cm^{-1}.

A UV-Vis spectrophotometer was used to analyze the stability and size of CuNPs-red dragon fruit peel extract nanoparticles by observing the absorbance of the CuNPs-red dragon fruit peel extract nanoparticle suspension in the wavelength range of 200 – 800 nm. Nanoparticle stability was determined based on the maximum absorbance consistency in time intervals of 0, 10, 20 and 30 minutes. The estimated particle size is determined using Equation 1.

$$d = \frac{\ln\left(\frac{\lambda_{SPR} - \lambda_0}{L_1}\right)}{L_2} \quad \ldots (1)$$

where d is the particle diameter, λ_{SPR} and λ_0 are the maximum and minimum wavelengths of *SPR*, respectively, L_1 = 6.53 and L_2 = 0.0216 are values taken from TEM vs UV-Vis data (Haiss *et al*. 2007).

A digital optical microscope was used to observe the surface morphology and pore size of *nata de coco*, CuNPs-red dragon fruit peel extract, and plasmonic films of *nata de coco*-CuNPs-red dragon fruit peel extract. Testing is carried out by placing the test sample on a glass slide, then observing its morphology using a digital optical microscope at 100× magnification.

The plasmonic film was then tested for its validity as a mercury sensor film using standard mercury solutions of 0.1, 0.3, 0.5, 0.7, and 0.9 ppm. Each film was dipped into a cuvette containing a standard mercury solution to measure its absorbance using a UV-Vis spectrophotometer at a maximum wavelength of 395.9 nm. The data obtained is then depicted as a graph of absorbance vs. concentration to obtain a calibration curve. The curve with the best linearity is validated to determine accuracy,

precision, limit of detections (LOD), limit of quantitations (LOQ), and measurement sensitivity as well as robustness and robustness of the measurement method.

The accuracy of UV-Vis spectrophotometric measurements was determined by repeatedly measuring the absorbance of the analyte and spike solutions for seven times (Nisa *et al*. 2020). Quantitatively, the accuracy value is determined by calculating % recovery (%*R*) using Equation 2.

$$\%R = \left(\frac{C_{analyte} + C_{spike} - C_{analyte}}{C_{spike}} \right) \times 100\% \ldots (2)$$

where C_{analit} is the analyte concentration and C_{spike} is the added spike concentration.

Precision is stated based on the repeatability of the absorbance measurement results using UV-Vis spectrophotometry from one of the standard test solutions carried out seven times. Referring to research by Hindayani & Hamin (2022), the precision value is determined based on the percent relative standard deviation (%RSD) value calculated using Equation 3.

$$\%RSD = \frac{SD}{\bar{x}} \times 100 \ldots (3)$$

where *SD* is standard deviation = $\sqrt{\frac{1}{N-1}\sum_{i=1}^{N}\left(x_i - \bar{x}\right)^2}$, x_i is the absorbance of one sample, $\bar{x}$ is the average absorbance, and *N* is the number/size of samples. A method is said to have good precision if it meets the % *RSD* criteria of less than 16 % (Pratiwi *et al.* 2016).

The sensitivity of UV-Vis spectrophotometric measurements is determined based on the slope value of the standard mercury solution calibration curve using Equation 4.

$$y = ax + b \ldots (4)$$

where *y* is the absorbance, *x* is the concentration of standard mercury solution, *a* is the slope, and *b* is the intercept for the absorbance vs. concentration.

The limit of detection (LOD) was determined using UV-Vis spectrophotometry by measuring the absorbance of a standard mercury solution with the lowest concentration in the calibration curve range for seven times by calculating using Equation 5.

$$\text{LOD} = X_{\text{average}} + 3\,SD \ldots (5)$$

where X_{average} is the average absorbance value and *SD* is the standard of deviation. The limit value of quantitation (LOQ) is calculated using Equation 6.

$$\text{LOQ} = X_{\text{average}} + 10\,SD \ldots (6)$$

The obtained LOD and LOQ absorbance values then converted into LOD and LOQ concentrations using the calibration curve equation $y = ax + b$.

The ruggedness and strength tests in this study are based on the similarity of the absorbance measurement results in the test solution which has been interacted with the plasmonic film under several different measurement conditions.

RESULTS AND DISCUSSION

The synthesis of *nata de coco* has been successfully carried out through the coconut water fermentation process using *Acetobacter xylinum* bacteria, where the *nata de coco* obtained is clean white in color, has a chewy and elastic texture resembling gel. Making *nata de coco* requires sufficient minerals, vitamins, carbon and nitrogen. Therefore, *nata de coco* is made by mixing coconut water, granulated sugar, Zwavelzur Ammonium (ZA), bacterial starter, and vinegar. Granulated sugar is a carbon source to meet the energy needs for bacterial growth so that nata formation is maximized. ZA is a source of nitrogen which functions to stimulate the growth and activity of *Acetobacter xylinum*, while the minerals and vitamins are sourced from coconut water itself.

The presence of a starter plays an important role in increasing the number of *Acetobacter xylinum* colonies that produce nata-forming enzymes. Referring to the research of Dirpan *et al*. (2019), the addition of vinegar aims to regulate the acidity or pH level to suit the characteristic conditions for optimum growth of *Acetobacter xylinum* bacteria, namely pH 4 and 5 at a temperature of 28℃ – 30℃. The formation of cellulose in the fermentation process begins with the appearance of thread-like fibers which then change shape into cellulose ropes like woven cellulose known as nata (Putri *et al*. 2021). The *nata de coco* formed is composed of a network of microfibrils. The membrane is formed as a result of a series of activities of the *Acetobacter xylinum* bacteria with the nutrients in the liquid media. Glucose nutrition is found in coconut water and granulated sugar. Glucose is formed by the hydrolysis reaction of sucrose with water in granulated sugar. The glucose involved in the formation of cellulose is β-glucose. α-Glucose is converted into β form by the isomerase enzyme in the *Acetobacter xylinum* bacteria. The change in β form occurs in the –OH group on the C-1 atom (Figure 1 (a). Next, glucose will bond with other glucose via a 1,4-β-glycoside bond. This bond occurs between the –OH group on the C-1 atom from one β-glucose with the –OH group on the C-4 atom of the other β-glucose (Figure 1 (b)). Different thicknesses at varying incubation times are related to the polymerization process.

Red dragon fruit obtained from the maceration process of peacock dragon fruit skin samples has a dark red-black color after evaporation with a yield value of 7.495% (Figure 2). Figure 2(a) shows the red dragon fruit extract before evaporation with black color, because the extract solution is concentrated

using a rotary evaporator at a temperature of 50°C for three hours. After evaporation in the oven at 50°C for 30 minutes, as shown in Figure 2(b), the color of the extract solution turned brown due to the loss of some of its water. Ethanol solvent was chosen in the maceration process because ethanol is relatively non-toxic compared to methanol, cheaper, easier to obtain, and not easily grown by fungi or bacteria. Ethanol itself is semipolar so it can attract secondary metabolite compounds in samples of red dragon fruit peel paste. The filtered filtrate was concentrated using a ratatory evaporator at a temperature of 50℃ for 3 hours at a speed of 123 millibars and a rotational speed of 120 rpm, to obtain a thick extract of red dragon fruit peel. Evaporation is carried out at low temperatures, because the secondary metabolite compounds in red dragon fruit peel extract are damaged when heated at temperatures above 50°C (Armanzah & Hendrawati 2016).

Synthesis of copper nanoparticles using the green synthesis method utilizes red dragon fruit peel extract as a bioreductant and 0.1 M $CuSO_4$ solution as a precursor. Suspension of CuNPs-red dragon fruit peel extract based on the composition of precursor: bioreductant with a volume ratio of 1:1 to 1: 6 is shown in Figure 3. As in previous research, variations in this composition aims to obtain a sufficient amount of bioreductant to reduce Cu^{2+} (Wisnuwardhani *et al*. 2019). The formation of CuNPs is characterized by a change in color from light blue to green which becomes increasingly darker as the bioreductant extract is added. However, the color change is not clearly visible visually. This color change can be analyzed by comparing the absorbance values obtained by UV-Vis spectroscopy, as shown in Figure 6. The higher the red dragon fruit peel extract volume, the higher the absorbance. According to Chandraker *et al*. (2020), the color change occurs due to ion deposition which shows the successful reduction of Cu^{2+} ions to CuNPs.

The anthocyanin compound in red dragon fruit peel extract reduces Cu^{2+} ions to Cu^0. The copper atoms formed tend to group together to form nanoparticles. When the maximum size of the nanoparticles is reached, CuNPs will try to attract anthocyanin compounds which act as capping agents to the surface of the nanoparticles to stabilize them, so that nanoparticle formation can stop and agglomeration can be avoided. The capping agent works through electrostatic interaction with CuNPs so that the cluster growth that occurs is not significant.

The anthocyanin compound in red dragon fruit peel extract can reduce Cu^{2+} ions because it has a hydroxyl group (–OH) which is able to donate an electron pair to Cu^{2+} ions. In addition, due to the release of hydrogen atoms by the hydroxyl group, the anthocyanin compound undergoes oxidation so that the hydroxyl group changes to a ketone group. Referring to the research by Haruna *et al*. (2022), the formation of CuNPs biosynthetically using anthocyanin compounds in red dragon fruit peel extract is proposed through a mechanism as shown in Figure 4. CuNPs-red dragon fruit peel extract is then inserted into the *nata de coco* cellulose matrix in making plasmonic film.

The use of *nata de coco* in making nanocomposites through the deposition of metal nanoparticles on the surface of *nata de coco* cellulose fibers has been previously reported (Salasa *et al*. 2016). Plasmonic films are made by using *nata de*

Figure 2. Red dragon fruit peel extract: (a) paste before evaporation and (b) after evaporation

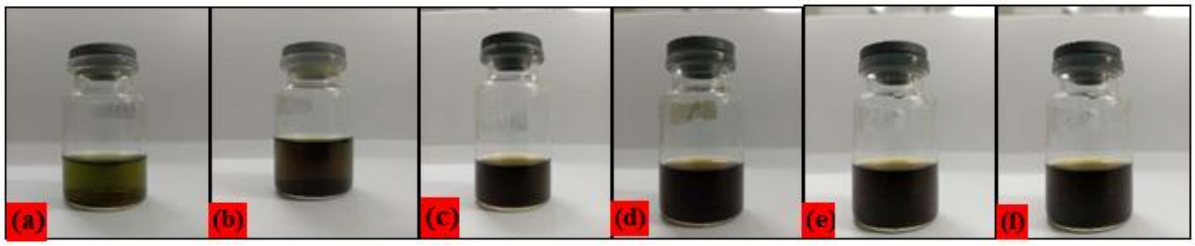

Figure 3. Changes in color of the mixture of Cu^{2+} precursor-red dragon fruit peel extract with a ratio of (a) 1:1, (b) 1:2, (c) 1:3, (d) 1:4, (e) 1:5, and (f) 1:6.

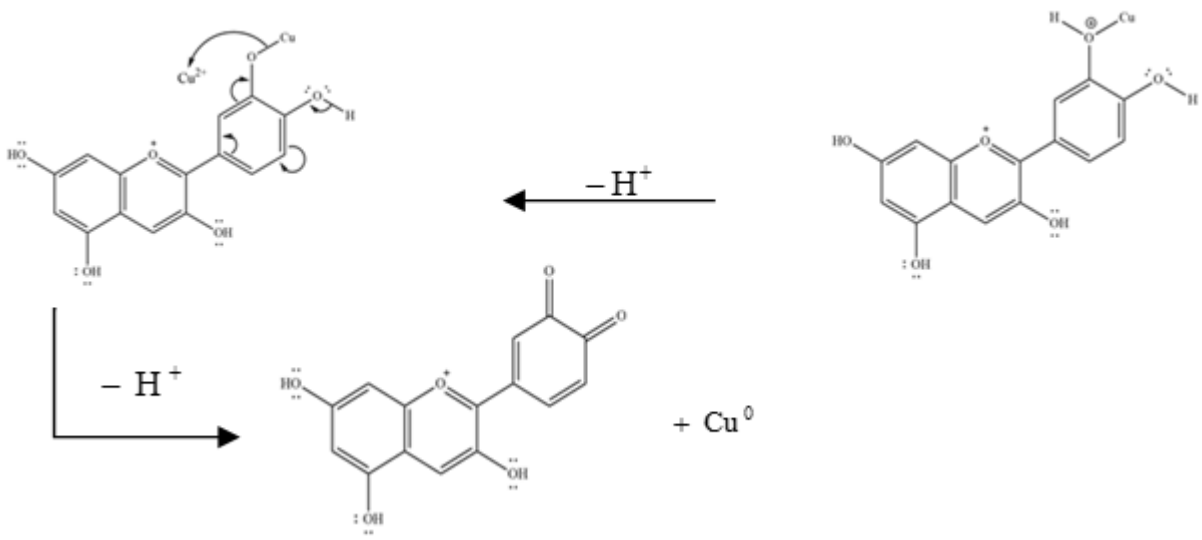

Figure 4. Proposed reaction mechanism for copper nanoparticles with anthocyanin compounds biosynthetically.

coco as a matrix, because *nata de coco* has a fibrous structure with a porous surface so that metal nanoparticles can be deposited in it.

The plasmonic film produced in this study has a green to yellowish color, corresponding to the color of the CuNPs suspension-red dragon fruit peel extract, which proves that CuNPs were deposited in the *nata de coco* film. The interaction of metal ions with *nata de coco* cellulose is thought to occur through electrostatic interactions of these cations with oxygen atoms in the hydroxyl groups which have lone electron pairs and ether groups in *nata de coco* cellulose to form complex compounds (Figure 5). This surface interaction can stabilize CuNPs. The advantage of this process is that the parent macromolecular chain plays a role in the synthesis and increased distribution of CuNPs in the cellulose matrix. In addition, these molecular chains prevent the formation of aggregates. At the same time, polymer chains play an important role in the narrow size distribution and well-defined shape of metal nanoparticles (Eivazihollagh *et al*. 2017).

In this research, characterization was carried out using a UV-Vis spectrophotometer, FTIR, and digital optical microscope. Characterization of the CuNPs filtrate-red dragon fruit peel extract using a UV-Vis spectrophotometer aims to determine the stability and estimate the particle size of the CuNPs obtained. The characterization of the dry residue aims to analyze functional groups and their changes as an indication of the formation of CuNPs-red dragon fruit peel extract. Characterization using a digital optical microscope aims for morphological analysis at 1000 times magnification.

Analysis using a UV-Vis spectrophotometer utilizes surface plasmon waves to observe the interactions that occur between Cu metal and bioreductor compounds. Analysis of the stability and size of the CuNPs formed was observed based on the radiation absorption pattern at a wavelength of 400 nm - 500 nm. Absorbance peaks in the time ranges of 0, 10, 20, and 30 minutes appeared at consistent wavelengths, indicating that the mixture of nanoparticles formed had good stability (Figure 6). The occurrence of a slight shift in the absorption peak to a larger wavelength indicates that the nanoparticles are relatively less stable due to agglomeration (Apriandanu *et al*. 2013). On the other hand, a shift in the absorption peak to a lower wavelength indicates that the interaction energy of CuNPs with the bioreductor compound has increased (Marslin *et al*. 2018). This is due to changes in the optical properties of CuNPs when the particles agglomerate and electrons approaching the particle surface experience delocalization and are shared with other particles, so that the SPR experiences a shift to a lower energy.

The results of analysis using FTIR show the presence of functional groups at wave numbers between 450 cm^{-1} – 4000 cm^{-1} (Figure 7). In Figure 10 (a), the absorption spectrum at wave number 3412.07 cm^{-1} shows the presence of an –OH group which is supported by the absorption of the alkane C–H bond at wave number 2929.87 cm^{-1}. Meanwhile, absorption at wave numbers 1722.43 cm^{-1}, 1620.20 cm^{-1}, and 1411.89 cm^{-1}, indicates the presence of the C=O group, alkene C=C bonds, and alkane C–H bonds, respectively. Next, peak absorption at 1078.20 cm^{-1} and 1041.56 cm^{-1} indicate the presence of C–O bonds.

When compared with the spectrum in Figure 7 (a), Figure 7 (b) shows a shift in wave number absorption for the –OH group (3439.07 cm^{-1}), C–H alkane (2922.15 cm^{-1}), C=O (1722.43 cm^{-1}), and C=C alkene (1652.99 cm^{-1}). The shift in the absorption peak from 3412.07 cm^{-1} to 3439.07 cm^{-1}

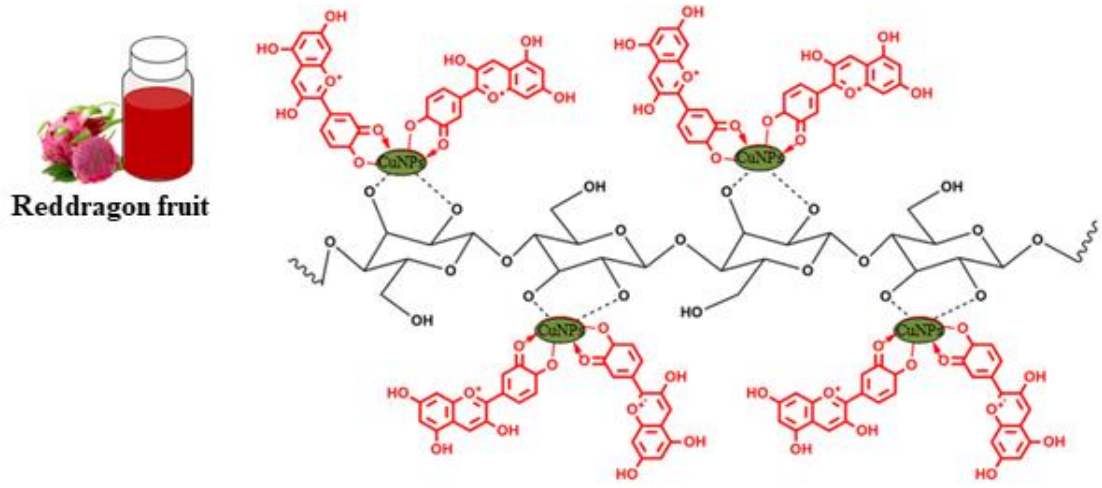

Figure 5. Illustration of the interaction of cellulose with CuNPs-red dragon fruit peel extract.

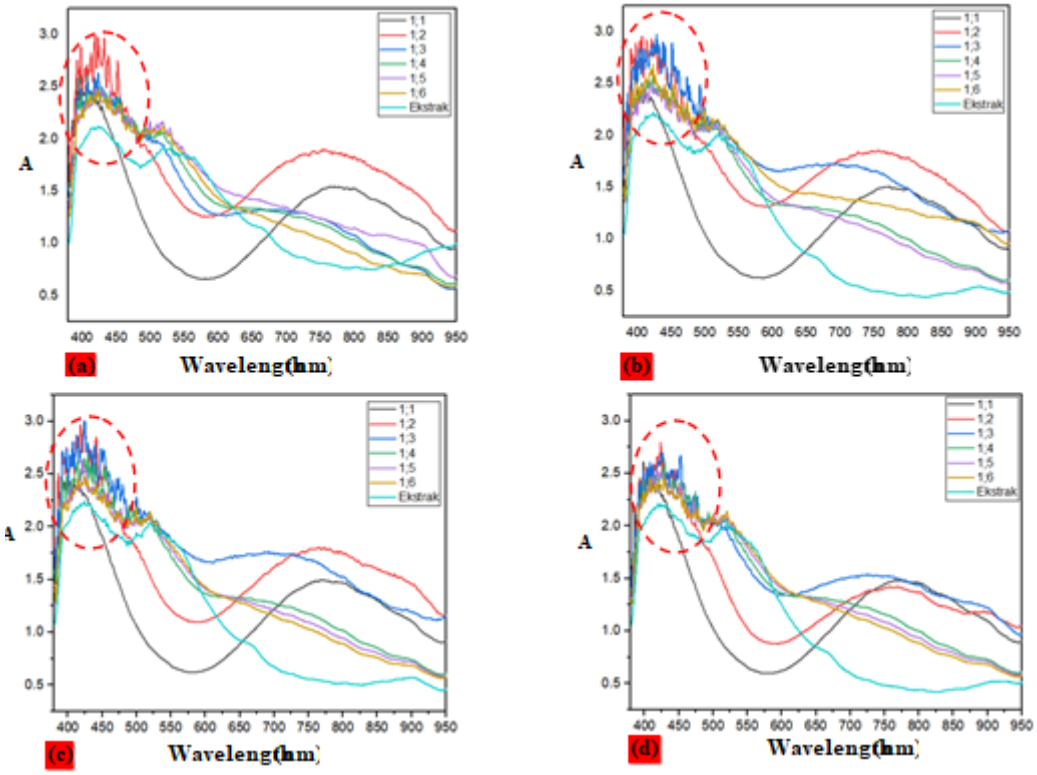

Figure 6. Absorbance (A) vs. wavelenght plots of UV-Vis radiation absorption of CuNPs-red dragon fruit peel extract at time intervals of (a) 0 minutes, (b) 10 minutes, (c) 20 minutes and (d) 30 minutes.

indicates the reduction of Cu^{2+} to form colloidal Cu^{0} nanoparticles (Kulkarni *et al*. 2014).

The spectrum in Figure 7 (c) shows a wide peak at wave number 3429.43 cm^{-1} for the –OH group due to stretching vibrations in the O-H bond. Absorption of IR radiation at a wave number of 2920.22 cm^{-1} shows the vibration of aliphatic C-H bonds. Absorption of IR radiation at wave numbers 1653 cm^{-1} and 1548.83 cm^{-1} indicates vibrations in the aromatic ring (Pratomo & Rohaeti 2011). The IR radiation at wave numbers 1489.04 cm^{-1} and 1055.06 cm^{-1} indicates the presence of C=O and C=C bonds.

The spectrum in Figure 8 (d) shows the shift in wave numbers at 3423.64 cm^{-1}, 2966.51 cm^{-1}, 2870.07 cm^{-1}, 1604.77 cm^{-1}, 1510.26 cm^{-1}, and 1521.20 cm^{-1} which indicates that interaction has occurred between nata de coco cellulose and CuNPs-red dragon fruit peel extract. This is reinforced by the absorption of IR radiation at a wave number of 667.37 cm^{-1} which indicates Cu-O interaction. The

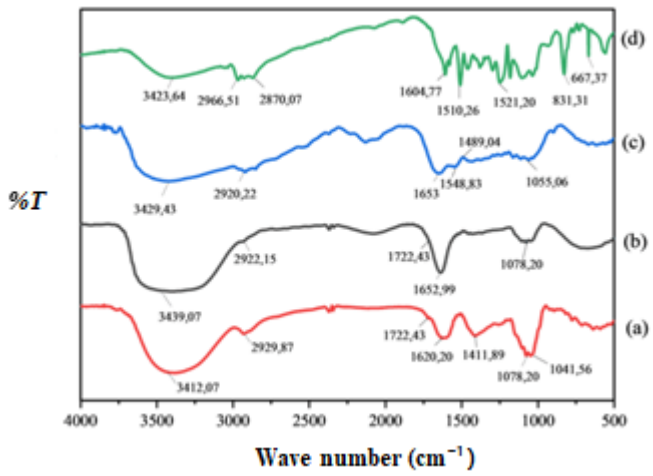

Figure 7. FTIR spectrum for: (a) red dragon fruit peel extract, (b) CuNPs-red dragon fruit peel extract, (c) Nata de coco, (d) plasmonic film-CuNPs-red dragon fruit peel extract.

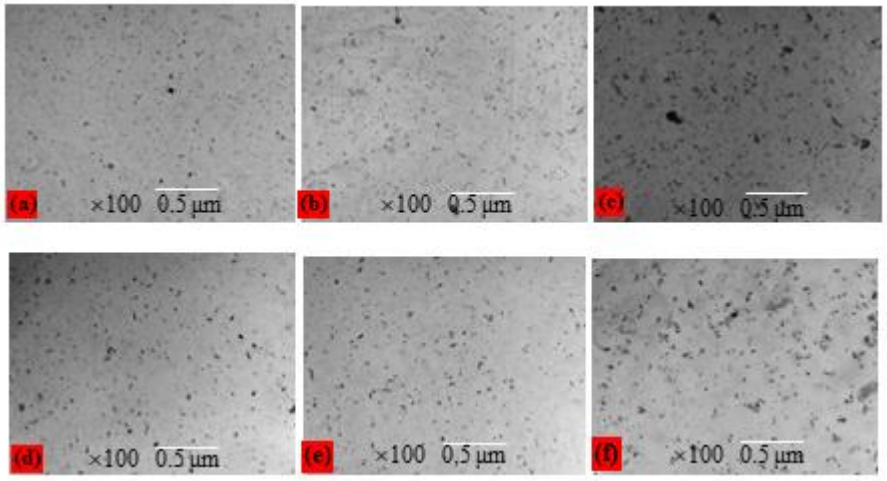

Figure 8 Morphology of CuNPs-red dragon fruit peel extract based on variations in the volume ratio of precursor: bioreductor (a) 1:1, (b) 1:2, (c) 1:3, (d) 1:4, (e) 1:5, and (f) 1:6, observed using a digital optical microscope with a magnification scale of 100 ×.

absorption peak at wave numbers 500 – 700 cm^{-1} indicates the vibration of the Cu–O bond.

The next characterization is determining the size of the nanoparticles. Referring to research by Masykuroh & Puspasari (2020), the size of the nanoparticles in this study was determined using a UV-Vis spectrophotometer based on SPR which is the characteristic of a material. The resonance peak of metal nanoparticles depends on the diameter of the nanoparticle and the refractive index of the surrounding medium. The absorption peak wavelength shifts to higher wavelengths as the nanoparticle size increases. The position of the plasmonic resonance peak has a quadratic dependence on the nanoparticle diameter. This shift occurs due to the reduction in the restoring force of electron oscillations when the size of the nanoparticles increases (Septriani & Muldarisnur 2022). The computational method for estimating the particle diameter of CuNPs was carried out by applying Equation 1. In this equation, the λ_{SPR} is taken from the maximum wavelength shown in Figure 6 which is in the range of 398.3 – 423.7 nm, as reported in previous studies (Marslin *et al*. 2018). The second peaks on the right are not the SPR wavelength of nanoparticles, but the wavelength peaks of other species that have not been detected. The particle size estimates obtained are presented in Table 1. This data shows that copper synthesized using $CuSO_4$ precursor and red dragon fruit peel extract bioreductor has reached a nanoparticle size, namely 1 – 100 nanometers.

Characterization using a digital optical microscope show that CuNPs-red dragon fruit peel extract have a uniform round shape. These results are in accordance with research by Haruna *et al*. (2022)

Table 1. Estimated size of CuNPs-red dragon fruit peel extract

Komposition of p:b	λ_{SPR}	λ_0	L_1	L_2	diameter (nm)
1:1	398.3	380.5	6.53	0.0216	46.43
1:2	407.5	380.5	6.53	0.0216	65.72
1:3	429.1	380.5	6.53	0.0216	92.93
1:4	423.7	380.5	6.53	0.0216	87.47
1:5	419.9	380.5	6.53	0.0216	83.21
1:6	423.7	380.5	6.53	0.0216	87.47

Note. p:b = precursors:bioreductors

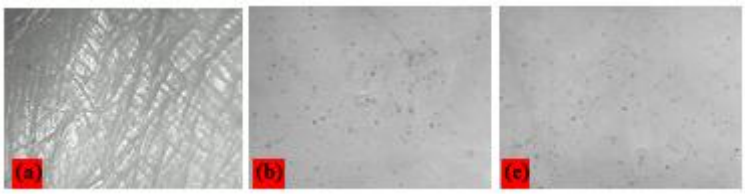

Figure 9. Morphology comparison of: (a) Nata de coco, (b) plasmonic film of nata de coco-CuNPs-red dragon fruit peel extract, and (c) plasmonic film of nata de coco-CuNPs-red dragon fruit peel extract-Hg.

which shows the uniformity of the particle size of the CuNPs obtained. CuNPs synthesized using $CuSO_4$ precursor and dragon fruit peel extract bioreductant in a ratio of 1:1 had the smallest size (Figure 8). This result is in accordance with the research of Willian *et al*. (2022) who synthesized CuNPs biosynthetically using a bioreductant from mangrove leaf extract. As red dragon fruit peel extract reducing agent was increased, the diameter of CuNPs slightly increased. This is assumed to be because a bioreductant concentration that is too high can increase the occurrence of nanoparticle agglomeration.

In the analysis of CuNPs deposition in cellulose membranes, it was seen that CuNPs-red dragon fruit peel extract had been deposited well on the membrane surface homogeneously. Figure 9 (a) shows that *nata de coco* has a fibrous structure and is quite homogeneous. Figure 9 (b) shows the shape or morphology of CuNPs which are deposited evenly on the surface of the plasmonic film of *nata de coco*-CuNPs-red dragon fruit peel extract. In addition, the particles suspected to be CuNPs were distributed more evenly throughout the plasmonic film (Figure 9 (c)). This film was further validated for determining mercury metal in samples using UV-Vis spectrophotometry.

Initial validation was carried out to obtain the coefficient of determination (R^2) for each plasmonic film. Measurement of the absorbance of a standard mercury solution using UV-Vis spectrophotometry in a cuvette containing a 1:1 plasmonic film produces a graph as shown in Figure 10. Calibration curve data for measuring standard mercury using a 1:1 – 1:6 plasmonic film is presented in Table 2.

The best curve linearity obtained in this study was found in 1:1 plasmonic fim with a R^2 value of 0.9935. An R^2 value close to 1 indicates a linear relationship between measured concentration and absorbance following the Lambert-Beer law. Measurement accuracy is determined based on the percent recovery value (%*R*) of the absorbance measurement results of standard analyte solutions by calculating using Equation 2. Accuracy values are acceptable if they range between 80-110% (Sahumena *et al*. 2020). Thus, the %*R* value obtained in this study shows very good measurement accuracy (Table 3).

Apart of accuracy, the measurement method must also have good precision as an illustration of the consistency of repeatability level of the measurement results. Statistically, the precision value is determined based on the relative standard deviation (%*RSD*) value using Equation 3. A test method is said to have a good degree of repeatability if the %*RSD* or precision value of ≤ 2% (Pratiwi *et al*. 2016). The %*RSD* data in Table 3 shows that the measurement method used has very good precision values so that it meets the measurement validity criteria.

The calibration curve can be used to determine the sensitivity of the test methode, namely the height of the absorbance value of an analyte with a low concentration. Therefore, the sensitivity test is carried out by determining the slope value of the standard mercury solution calibration curve as shown in Figure 10. A large slope value indicates that the measurement method applied has very good sensitivity.

Based on Equation 4, the slope value obtained for measuring standard mercury by UV-Vis spectrophotometry using a 1:1 plasmonic film has the greatest sensitivity, namely 1.5083. The slope value can also provide an idea of the effectiveness of the method being tested, namely by comparing it with the

Table 2. Validity parameters of plasmonic film calibration curves

Film Code	Regretion Equation	Concentration Range (ppm)	Linierity (R^2)	Sensitivity (slope)
1:1	$y = 1.5083x - 0.0368$	0.2 – 0.6	0.993	1.5083
1:2	$y = 0.1230x + 0.0500$	0.2 – 0.6	0.987	0.1230
1:3	$y = 0.1190x + 0.0490$	0.2 – 0.6	0.981	0.1190
1:4	$y = 0.1230x + 0.0570$	0.2 – 0.6	0.989	0.1230
1:5	$y = 0.1190x + 0.0320$	0.2 – 0.6	0.969	0.1190
1:6	$y = 0.1250x + 0.0380$	0.2 – 0.6	0.974	0.1250
Without Film	$y = 0.1370x + 0.0760$	0.2 – 0.6	0.958	0.1370

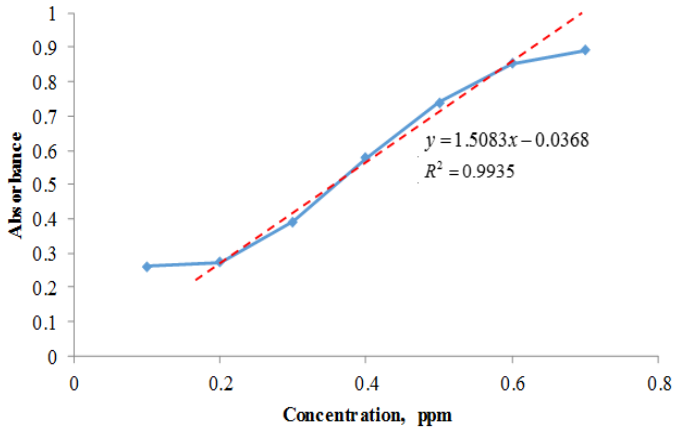

Figure 10 Graph of absorbance measurement of standard mercury solutions UV-Vis spectrophotometrically using 1:1 plasmonic film.

Table 3. Validity Method

Measurements Repetition	Absorbance of 0.2 ppm Hg Standard Solution		Absorbance of 0.2 ppm Hg Standard Solution + Spike
1	0.2131		0.2123
2	0.2421		0.2328
3	0.2218		0.2268
4	0.2103		0.2303
5	0.2123		0.2381
6	0.2112		0.2411
7	0.2321		0.2221
Average	0.2204		0.2291
SD	0.011434837567892		
%*R*			103.9%
%*RSD*	0.9%		
LOD = Average + 3 *SD*	0.2547	0.193 ppm	
LOQ = Average + 10 *SD*	0.33478	0.245 ppm	

Table 4. %*RSD* Values for Varying Measurement Times of 0, 30, 60, 90 and 120 Minutes

Measurement time (minutes)	Absorbance							%*RSD*
	1	2	3	4	5	6	7	
0	0.3680	0.3931	0.5193	0.6225	0.6548	0.6785	0.7372	1.0%
30	0.3510	0.3852	0.5695	0.6425	0.6835	0.6953	0.7572	1.2%
60	0.3610	0.3932	0.5293	0.6125	0.6648	0.7285	0.7672	1.0%
90	0.3810	0.3924	0.5393	0.6525	0.6948	0.7586	0.7972	1.2%
120	0.4410	0.4925	0.5695	0.6525	0.6848	0.7786	0.8672	1.0%

slope value measured without using a plasmonic film. Without using a plasmonic film, the slope value obtained is 0.137. In addition, the very low intercept value is close to zero, namely –0.0368, indicating that the presence of the plasmonic film is able to prevent the absorption of visible radiation by non-analyte species. Measurement of mercury by UV-Vis spectrophotometry in cuvettes containing plasmonic films is more sensitive than those without plasmonic films with the same other validation parameters.

A measurement feasibility test that is no less important is determining the limit of detection (LOD) and limit of quantitation (LOQ). The determination of LOD and LOQ in this study was based on absorbance measurements obtained from plasmonic film measurements under 7 repetitions. By using Equation 5 and Equation 6 which have been converted into the equation $y = 1.5083x - 0.0368$, the x values are obtained as LOD and LOQ (Table 3). Based on the LOD value, it can be said that the lowest mercury concentration that can still be detected and measured significantly is 0.193 ppm. This value is still below the permitted threshold for the heavy metal mercury, namely 0.50 ppm. Based on the LOQ value, it can be said that the smallest quantity of mercury analyte that still meets the criteria for accuracy and precision in UV-Vis spectrophotometric measurements is 0.246 ppm.

Toughness and strength tests in this study were carried out by comparing the %*R* value of the results of measuring the absorbance value of standard mercury using UV-Vis spectrophotometry in cuvettes containing plasmonic film at different times, namely at 0 minutes, 30 minutes, 60 minutes, 90 minutes, and 120 minutes under 7 repetitions. This measurement data is presented in Table 4. The results of this test show that the absorbance value obtained did not experience significant changes under 7 repetitions and met the valid %*RSD* value, namely ≤ 2%. These measurement results prove that the plasmonic film provides good toughness and measurement strength, because it is not affected by test variations given during the measurement.

Furthermore, by using the standard mercury solution calibration curve, the results of UV-Vis spectrophotometric measurements using a cuvette containing the best plasmonic film, namely 1:1 plasmonic film, obtained an absorbance of the test sample solution of 0.314. Thus, by entering the value 0.314 as y into the equation: $y = 1.5083x - 0.0368$, we obtain the value of x as the concentration of mercury in the sample of 0.233 ppm. This value has exceeded the permitted threshold value for mercury, namely 0.5 ppm. In this test, the brownish green color of the plasmonic film before interacting with the mercury sample experienced color fading after interacting with the mercury sample.

CONCLUSION

In this research, a plasmonic film based on *nata de coco* cellulose inserted with Cu nanoparticles and dragon fruit peel extract has been successfully synthesized to detect mercury metal in samples. Characterization results using a UV-Vis spectrophotometer indicated the formation of stable copper nanoparticles with an RPS wavelength of 398.3 – 423.7 nm. Characterization using a UV-Vis spectrophotometer also showed the successful synthesis of copper nanoparticles with an estimated nanoparticle size of 46.43 nm – 87.47 nm with a uniform round particle shape. The characterization using FTIR shows a change in the spectrum peak of the –OH group from wave number 3412.07 cm^{-1} to wave number 3439.07 cm^{-1} which indicates that a redox reaction occurred in the formation of Cu nanoparticles between the functional groups in the bioreductor compound and the precursor $CuSO_4$. The obtained *nata de coco* cellulose film inserted with Cu nanoparticles-dragon fruit peel extract was proven to be suitable as a plasmonic sensor for the determination of mercury metal with an accuracy value (%*R*) of 103.9%, precision (%*RSD*) of 0.9%, LOD of 0.193 ppm, LOQ of 0.245 ppm, and sensitivity of 1.50, and has good toughness and strength for repeated measurements at varying times. Based on a comparison of the sensitivity values, measurements using a plasmonic film were proven to be more sensitive than without using a plasmonic film. To complement the reliability of plasmonic film for the detection of mercury metal using UV-Vis

spectrophotometry, it is necessary to test its effectiveness with other parameters such as the linearity of the calibration curve, the measurement concentration range and the limit of detection.

ACKNOWLEDGMENTS

Thanks so much we express to the Directorate of Learning and Student Affairs, Director General of Higher Education, Ministry of Education, Culture, Research and Technology, Republic of Indonesia as fund provider with contract number 005/E2/PPK/SPPK/PKM/2022.

REFERENCES

Al-ayubi, M.C., Barroroh, H. & Dewi, D.C. (2010). Studi keseimbangan adsorpsi merkuri (II) pada biomassa daun enceng gondok (eichhornia crassipes). *ALCHEMY: Journal of Chemistry*. **1(2)**: 53-103.

Amaliyah, R., Kristiningrum, R. & Sary, I.P. (2021). Pengembangan sensor kimia berbasis strip tes untuk deteksi logam berat merkuri pada sampel produk jamu. *E-Journal Pustaka Kesehatan*. **9 (1)**:25-33.

Apriandanu, D.O B., Wahyuni, S. & Hadisaputro, S. (2013). Sintesis nanopartikel perak menggunakan metode poliol dengan agen stabilisator polivinilalkohol (PVA). *Indonesian Journal of Mathematics and Natural Sciences.* **36(2)**: 157-168.

Armanzah, R.S. & Hendrawati, T.Y. (2016). Pengaruh waktu maserasi zat antosianin sebagai pewarna alami dari ubi jalar ungu (*Ipomoea batatas* L. Poir). *In Seminar Nasional Sains dan Teknologi*. Jakarta. 8 November 2016. pp. 1-10.

Boby, C.A., Roni, A. & Muhsinin, S. (2021). Review: produksi, karakterisasi dan aplikasi selulosa bakteri di bidang farmasi, *Journal of Pharmacy and Science (JOPS)*. **4(2)**: 12-28.

Chandraker, S.K., Lal, M. & Shukla, R. (2019). DNA-binding, antioxidant, H_2O_2 sensing and photocatalytic properties of biogenic silver nanoparticles using Ageratum conyzoides L. leaf extract. *RSC Advances*. **9(40)**: 23408-23417.

Dirpan, A., Kamaruddin, I., Syarifuddin, A., Zainal., Rahman, A.N.F., Hafidzah., Latief, R. & Prahesti, K.I. (2019). Characteristics of bacterial cellulose derived from two nitrogen sources: ammonium sulphate and yeast extract as an indicator of smart packaging on fresh meat. *IOP Conference Series: Earth and Environmental Science*. **355(1)**: 1-7.

Eivazihollagh, A., Bäckström, J., Dahlström, C., Carlsson, F., Ibrahem, E., Lindman, B., Edlund, H. & Norgren, M. (2017). One-Pot synthesis of cellulose-templated copper nanoparticles with antibacterial properties. *Materials Letters*. **187**: 170–172.

Haiss, W., Thanh, N.T., Aveyard, J. & Fernig, D. G. (2007). Determination of size and concentration of gold nanoparticles from UV−Vis spectra. *Analytical Chemistry*. **79(11)**: 4215-4221.

Haruna, C.A., Malik, W.A., Rijal, M.Y.S., Watoni, A.H. & Ramadhan, L.O.A.N. (2022). Green synthesis of copper nanoparticles using red dragon fruit (*Hylocereus polyrhizus*) extract and its antibacterial activity for liquid disinfectant. *Jurnal Kimia Sains dan Aplikasi*. **13(25)**: 352-361.

Hasriana. (2021). Sintesis dan karakterisasi komposit nata de coco perak fosfat (Ag_3PO_4)-ekstrak kulit buah naga merah (*Hylocereus polyrhyzuz*) untuk filter pada masker antimikroba. Skripsi. Fakultas Matematika & Ilmu Pengetahuan Alam. Universitas Halu Oleo. Kendari.

Hindayani, A. & Hamim, N. (2022). Akurasi dan presisi metode sekunder pengukuran konduktivitas menggunakan sel jones tipe e untuk pemantauan kualitas air minum. *Indonesian Journal of Chemical Analysis (IJCA)*. **5(1)**: 41-51.

Kulkarni, V. & Kulkarni, P. (2014). Synthesis of copper nanoparticles with aegle marmelos leaf extract. *Nanosci Nanotechnol*. **8**: 401-404.

Laila, P.V.Z., Tegar, T. & Perdana, F. (2021). Studi awal sintesis nanopartikel menggunakan bioreduktor ekstrak daun ketapang (*Terminalia catappa*). *Photon Jurnal Sains dan Kesehatan*. **12(1)**: 78-83.

Marslin, G., Siram, K., Maqbool, Q., Selvakesavan, R.K., Kruszka, D., Kachlicki, P. & Franklin, G. (2018). Secondary metabolites in the green synthesis of metallic nanoparticles. *Materials*. **11(6)**: 940.

Masykuroh, A., & Puspasari, H. (2020). Potensi tanaman keladi sarawak *Alocasia macrorrhizos* dalam biosintesis nano partikel perak (Nnp): Analisis *Surface Plasmon Resonance* (SPR) sebagai fungsi waktu. *Bioma: Jurnal Biologi Makassar*. **5(2)**: 233-240.

Miftahurrahmah, Suhendrayatna, Zaki, M. (2017). Penyisihan ion logam merkuri (Hg^{2+}) menggunakan adsorben berbahan baku limbah pertanian dan gulma tanaman. *Jurnal Teknik Kimia USU*. **6(1)**: 7-11.

Nisa, C., Saputra, P. & Setiawati, E. (2020). Pengembangan dan validasi metode uji cadmium pada air permukaan secara spektrofotometri serapan atom nyala. In Prosiding Pertemuan dan Presentasi Ilmiah Standarisasi. Tangerang. 5 November 2020. pp. 249-258.

Oh, S.Y., Lee, M.J., Heo, N.S., Kim, S., Oh, J.S., Lee, Y., Jeon, E. J., Moon, H., Kim, H. S., Park, T. J., Moon, G., Chun, H. S. & Huh, Y.S. (2019b). Cuvette-Type LSPR sensor for highly sensitive detection of melamine in infant formulas. *Sensors*. **19(18)**: 3839.

Pratiwi, L., Fudholi, A., Martien, R. & Pramono, S. (2016). Ethanol extract, ethyl acetate extract, ethyl acetate fraction, and n-heksan fraction mangosteen peels (*Garcinia mangostana* L.) as source of bioactive substance free-radical scavengers. *JPSCR: Journal of Pharmaceutical Science and Clinical Research*. **1(2)**: 71-82.

Pratomo, H., & Rohaeti, E. (2011). Bioplastik Nata de Cassava as Material Edible Film Environmentally Friendly. *Jurnal Penelitian Saintek*. **16(2)**: 172-190.

Putri, S.N.Y., Syaharani, W.F., Utami, C.V.B., Safitri, D.R., Arum, Z.N., Prihastari, Z.S. & Sari, A.R. (2021). The Effect of microorganism, raw materials, and incubation time on the characteristic of nata: A Review. *Jurnal Teknologi Hasil Pertanian*. **14(1)**: 62-74.

Rahmawati, N.H., Islam, A.I. & Kurniawati, R. (2020). Smart biosensor berbasis emas-nanopartikel sebagai teknologi mutakhir deteksi penyakit triple burden disease. *Journal of the Indonesia Scientific Society (JISS)*. **1(1)**: 1-10.

Sahumena, M.H., Ruslin, R., Asriyanti, A. & Djuwarno, E.N. (2020). Identifikasi jamu yang beredar di kota Kendari menggunakan metode spektrofotometri UV-Vis. *Journal Syifa Sciences and Clinical Research (JSSCR)*. **2(2)**: 65-72.

Salasa, D., Aritonang, H. & Kamu, V.S. 2016. Sintesis nanopartikel perak (Ag) dengan reduktor natrium borohidrida (NaBH4) menggunakan matriks nata de coco. *Chemistry Progress*. **9(2)**: 34-40.

Septriani, Y. & Muldarisnur, M. (2022). Kontrol ukuran nanopartikel perak dengan variasi konsentrasi ekstrak kulit buah manggis. *Jurnal Fisika Unand*. **11(1)**: 68-74.

Setiyono, A. & Djaidah, A. (2012). Konsumsi ikan dan hasil pertanian terhadap kadar Hg darah. *Jurnal Kesehatan Masyarakat*. **7(2)**: 110-116.

Silalahi, I.H., Zahara, T.A. & Tampubolon, H.M. (2012). Kapasitas adsorpsi merkuri menggunakan adsorben *Sargassum crassifolium* teraktivasi. *Biopropal*. **3**: 28-38.

Widianingsih, M. (2017). Aktivitas antioksidan ekstrak metanol buah naga merah (*Hylocereus polyrhizus* (FAC Weber) Britton & Rose) hasil maserasi dan dipekatkan dengan kering angin. *Jurnal Wiyata: Penelitian Sains dan Kesehatan*. **3(2)**: 146-150.

Willian, N., Syukri, S., Zulhadjri, Z., Pardi, H. & Arief, S. (2022). Marine plant mediated green synthesis of silver nanoparticles using mangrove *Rhizophora stylosa*: Effect of variable process and their antibacterial activity. *F1000Research*. **10**: 768.

Wisnuwardhani, H.A., Roosma, A., Lukmayani, Y., Arumsari, A. & Sukanta, S. (2019). Optimasi kondisi sintesis nanopartikel tembaga menggunakan ekstrak biji melinjo (*Gnetum gnemon* L.). *JIIS (Jurnal Ilmiah Ibnu Sina): Ilmu Farmasi dan Kesehatan*. **4(2)**: 353-360.

Yanty, Y.N. & Siska, V.A. (2017). Ekstrak kulit buah naga merah (*Hylocereus polyrhizus*) sebagai antioksidan dalam formulasi sediaan lotion. *Jurnal Ilmiah Manuntung: Sains Farmasi dan Kesehatan*. **3(2)**: 166-172.

Zaki, M. (2017). Penyisihan ion logam merkuri (Hg^{2+}) menggunakan adsorben berbahan baku limbah pertanian dan gulma tanaman. *Jurnal Teknik Kimia USU*. **6(1)**: 7-11.